The EUMETSAT
Network of
Satellite
Application
Facilities

ROM SAF
Radio Occultation Meteorology

ROM SAF CDOP-2

Visiting Scientist Report 22:

Beta testing of ROPP 7.0

Torsten Schmidt

Danish Meteorological Institute (DMI)
European Centre for Medium-Range Weather Forecasts (ECMWF)
Institut d'Estudis Espacials de Catalunya (IEEC)
Met Office (METO)

Ref: SAF/ROM/DMI/REP/VS22/001
Version: 1.0
Date: 7 June 2013

DOCUMENT AUTHOR TABLE

	Author(s)	Function	Date	Comment
Prepared by:	Torsten Schmidt	ROM SAF Visiting Scientist	07/06/2013	
Reviewed by (internal):	Ian Culverwell	ROM SAF Project Member	07/06/2013	
Approved by:	Kent B. Lauritsen	ROM SAF Project Manager	09/06/2013	

DOCUMENT CHANGE RECORD

Issue/Revision	Date	By	Description
Draft 1	27/05/2013	TS	First draft
Final version	07/06/2013	TS	Final report

VS Author

This VS study was carried out by Dr. Torsten Schmidt, Helmholtz Centre Potsdam, GFZ German Research Centre for Geosciences, Potsdam, Germany; Email: tschmidt@gfz-potsdam.de

VS Duration

The VS study was performed during May 2013 at the home institute of the candidate.

ROM SAF

The Radio Occultation Meteorology Satellite Application Facility (ROM SAF) is a decentralised processing center under EUMETSAT which is responsible for operational processing of GRAS radio occultation data from the Metop satellites and radio occultation (RO) data from other missions. The ROM SAF delivers bending angle, refractivity, temperature, pressure, and humidity profiles in near-real time and offline for NWP and climate users. The offline profiles are further processed into climate products consisting of gridded monthly zonal means of bending angle, refractivity, temperature, humidity, and geopotential heights together with error descriptions.

The ROM SAF also maintains the Radio Occultation Processing Package (ROPP) which contains software modules that will aid users wishing to process, quality-control and assimilate radio occultation data from any radio occultation mission into NWP and other models.

The ROM SAF Leading Entity is the Danish Meteorological Institute (DMI), with Cooperating Entities: i) European Centre for Medium-Range Weather Forecasts (ECMWF) in Reading, United Kingdom, ii) Institut D'Estudis Espacials de Catalunya (IEEC) in Barcelona, Spain, and iii) Met Office in Exeter, United Kingdom. To get access to our products or to read more about the ROM SAF please go to: http://www.romsaf.org

List of Contents

Executive Summary

The objectives of this study are to install, assess and report on the ease of use, capability and usefulness of the seventh major release of the Radio Occultation Processing Package, ROPP-7.0. The main focus is to assess the robustness and scientific integrity of the ROPP tropopause height (TPH) diagnostic tools.

The mainly used package for this activity was the pre-processor module. The according user guide is well structured and the main components of the tool are well documented. The installation of the ROPP-7.0 packages on a local machine was easy.

The focus in this study was on the new developed TPH diagnostic tools giving the possibility to calculate the TPH on the basis of bending angle, refractivity, dry temperature, and temperature. The idea to include these diagnostics is well-founded because about one decade ago it was recognised that the tropopause height is a suitable tool for the detection of climate change (Santer et al., 2004). In the meantime several studies using radio occultation (RO) data demonstrated already an increase of the global TPH by about 70 m over the last decade (e.g. Schmidt et al., 2008; 2010).

In this study the different TPH diagnostic tools were tested with a one-month Metop-A GRAS NRT dataset for April 2013 (over 19 000 occultation events). Based on this dataset a zonal climatology (10° latitude bins) was generated to evaluate the results from a climatological perspective. In addition to that one month (April 2013) of GRACE-A and TerraSAR-X data (about 10 000 occultations) processed at GFZ Potsdam was used to calculate the TPH on the basis of an own and independent method. A similar zonal climatology was provided.

The main results of the study are:

- Mean TPHs based on refractivity and (dry) temperature agree within 500 m for nearly all latitude bands including the GFZ data based on dry temperatures.
- The TPH based on bending angle is about 1 km higher compared with the other TPHs for all latitude bands.
- The yield of profiles with calculated TPHs however is generally low for TPHs based on bending angle, refractivity and dry temperature:
    - 59.4% for TPH based on bending angle (in the following called TPH_BEND),
    - 43.3% for TPH based on refractivity (in the following called TPH_REFR),
    - 39.6% for TPH based on dry temperature (in the following called TPH_TDRY).
- The cold-point tropopause from dry temperatures (CPT_TDRY in the following) gives partly unrealistic heights in all latitude bands and should be revised.

1. Introduction

1.1 Purpose of Document

This document contains the results from the ROM SAF Visiting Scientist activity with focus on a review about different TPH diagnostic tools based on bending angle, refractivity, dry temperature, and temperature.

The document is organized as follows: Chapter 2 contains general points regarding the download, installation, and documentation of the ROPP-7.0 software package. In Chapter 3 the different TPH diagnostic tools are reviewed. Chapter 4 contains some conclusions and finally in Chapter 5 some references are listed.

1.2. The tropopause height as climate change parameter

The upper troposphere and lower stratosphere (UTLS) region is one of the key regions of the atmosphere with important links to the stratosphere-troposphere exchange as well as climate research. The determination of UTLS temperature and tropopause height trends are crucial for the monitoring of climate change processes. The global mean tropopause height, e.g., shows an increase in reanalyses and radiosonde observations during the last decades (Seidel and Randel, 2006), whereas an upper tropospheric warming and a lower stratospheric cooling is evident (Randel et al., 2009). The changes in the tropopause height are caused by different forcing mechanisms (Shepherd, 2002). One mechanism leading to an increase of the tropopause height is a warming of the troposphere (due to more CO_2) and a cooling of the lower stratosphere (due to less stratospheric ozone), both observed during the last decades.

Lewis (2009) introduced a new method for the identification of TPHs from GPS radio occultation (RO) bending angles. Schmidt et al. (2010) demonstrated already an increase of the global tropopause height by about 70 m over the last decade associated with a tropospheric warming and a lower stratospheric cooling on the basis of RO data since 2001.

Therefore the continuous monitoring of the tropopause height is an important goal in atmospheric and climate research and operational tools for the detection of the tropopause are of largely scientific integrity.

2. General assessment of ROPP-7.0

2.1 Download of beta release of ROPP-7.0, and associated documentation from the ROM SAF website

No major issues have been detected during the download of ROPP-7.0 and the associated documentation from the ROM SAF website.

2.2 Report on ease of installation, the quality of the documentation, the general utility of the package, and any specific difficulties encountered

No major issues have been detected during the local installation of ROPP-7.0.

The installation of the ROPP-7.0 packages was performed on the following system/machine with the according parameters/compiler:

- CPU: Intel® Core™ i7-3770, 3.4 GHz,
- OS: Linux 3.4.28-20.2 desktop x86_64,
- System: OpenSUSE 12.2 x86_64, KDE 4.8.5 “release 2”,
- Compiler: gfortran

The overall installation process was easy based on the description files (e.g. README) and the buildpack package. The mainly used package for this activity was the pre-processor module.

The according user guide is well structured and the main components of the tool are well documented.

3. Scientific assessment of TPH diagnostic

3.1 Assess robustness of ROPP TPH diagnostic by passing through large amounts of data

A one-month GRAS dataset for April 2013 (over 19 000 occultation events) was provided as a test dataset for the TPH evaluation. The dataset consists of two parts containing bending angle and refractivity information (atm) and temperature from co-located ECMWF background profiles (bgr):

- atm20130401_000212_M02_2030483900_N0019_XXXX.nc (single sample file)
- bgr20130401_000212_M02_2030483900_N0019_XXXX.nc (single sample file)

From the atm files dry temperatures were calculated using the stand alone invert tool (see below). For the calculation of the different TPHs the “ropp_pp_tph_tool” program was applied to each individual GRAS data file:

- ropp_pp_tph_tool -o outputfile1 -d inputfile
- ropp_pp_invert_tool inputfile -mfile MSIS_coeff.nc -c romsaf_invert.cf -m GMSIS -d -o outputfile2
- ropp_pp_tph_tool -o outputfile3 -d outputfile2
- ropp_pp_tph_tool -o outputfile4 -c -d outputfile2

with inputfile = atmfile
outputfile1 contains TPH_BEND and TPH_REFR
outputfile2 contains dry temperatures based on inputfile
outputfile3 contains TPH_TDRY
outputfile4 contains CPT_TDRY

and

- ropp_pp_tph_tool -o outputfile3 -d inputfile
- ropp_pp_tph_tool -o outputfile4 –c -d inputfile

with inputfile = bgrfile
outputfile3 contains the TPH_TEMP
outputfile4 contains the CPT_TEMP

No major issues have been detected by passing through the large amount of data.

Recommendation: Give the CPT output in parallel to the TPH output. This spares the second run of the THP tool with the –c option.

In addition to the GRAS data one month (April 2013) of GRACE-A and TerraSAR-X dry temperature data (about 10 000 occultations) processed at GFZ Potsdam was used to calculate the TPH/CPT on the basis of an own and independent method.

3.2 Assess the scientific integrity of the ROPP TPH diagnostic by comparing and contrasting with alternative independent methods and measures

3.2.1 General overview

For a first (climatological) overview all calculated individual TPHs are plotted according their latitude and a zonal climatology (10° latitude bins centred at 85°S, 75°S, …, 75°N, 85°N) was generated to test the results from a climatological perspective (Figure 1).

The main properties from Figure 1 are:

- Generally there is a good agreement between the different TPHs and they are reasonable in a climatological sense.
- The variation of TPH_BEND (Figure 1a) is largest compared with the other TPHs.
- The number of successful processed TPHs differs considerable with lowest values for the dry temperature TPH.

For TPH_TDRY in the extra-tropics it is apparent (Figure 1c) that the TPH is not lower than 7 km caused by an according condition/restriction in the THP_TDRY routine. From other studies it is well-known that (individual) TPHs can be lower than 7 km in these regions. Also the other TPHs based on bending angle, refractivity, and temperature show TPHs less than 7 km in the extra-tropics. This will be further discussed in Chapter 3.2.4.

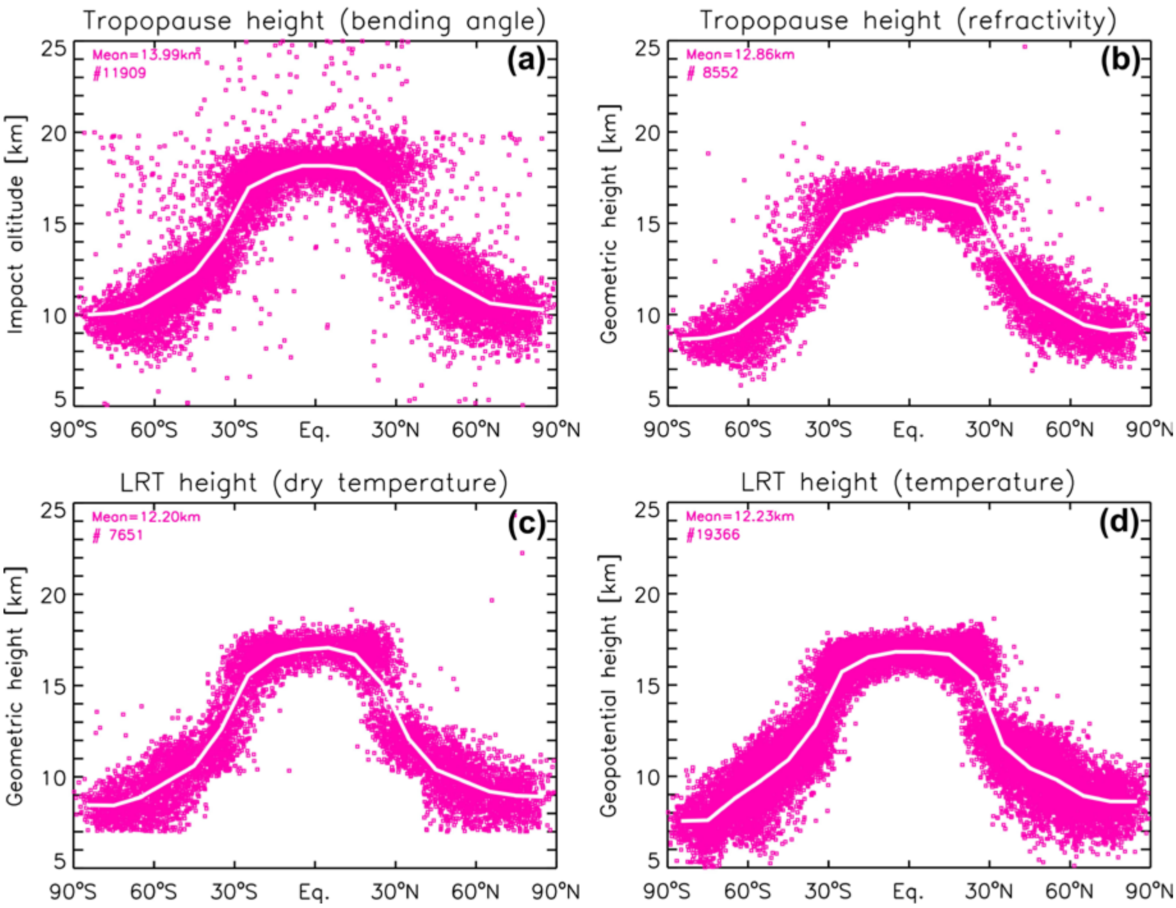

Figure 1: Tropopause heights from GRAS RO for April 2013 based on different datasets. (a) bending angle, (b) refractivity, (c) lapse-rate tropopause (LRT) from dry temperatures, and (d) same as (c), but for temperatures. The solid white lines denote the mean values for 10° latitude bins.

In comparison to the GFZ GRACE-A and TerraSAR-X dry temperature TPHs the agreement is very good (Figure 2), but the number of valid TPHs from the GFZ dataset is much higher. From only 39.6% (related to the total number of profiles) of the GRAS profiles a valid TPH_TDRY could be estimated. In contrast only from 2 single profiles from more than 10 000 profiles of the GFZ dataset a TPH_TDRY could not be calculated.

The reason for the low yield of the GRAS data is probably caused by the retrieval software generating the dry temperatures where most of the profiles do not reach the middle troposphere. A more detailed discussion is given in Chapter 3.2.4.

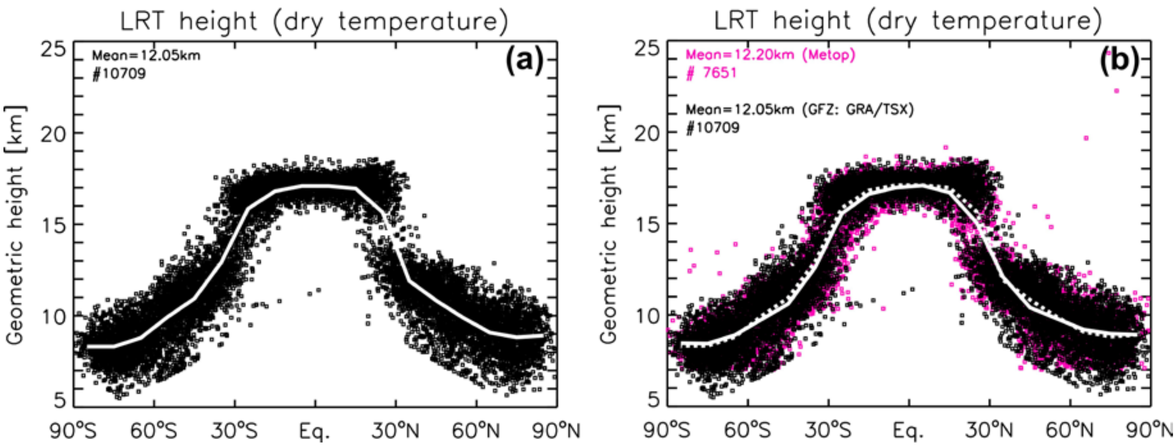

Figure 2: (a) Tropopause heights from GFZ GRACE-A and TerraSAR-X dry temperatures for April 2013. (b) Same as (a), but with GRAS TPHs (red) from Figure 1c. The white lines denote the mean values for 10° latitude bins (solid: GFZ, dotted: GRAS).

The CPT heights from the (dry) temperatures are presented in Figure 3. The CPT_TDRY (Figure 3a) shows a large spread with several unrealistic values in all latitude bands.

From a scientific point of view the concept of the cold-point tropopause is only reasonable in the tropics (Highwood and Hoskins, 1998; Fueglistaler et al., 2009). In the deep tropics (15°N-15°S) the CPT height is about 0.5 km above the lapse-rate tropopause (e.g. Schmidt et al., 2004) as shown by the additional GFZ CPT heights in Figure 3.

On the other hand the detection of the minimum temperature and the according height in a temperature profile (not restricted to 25 km) could be useful, e.g. in the polar vortex region during winter. According the minimum temperatures within the vortex the conditions for ozone destruction in spring could be formed.

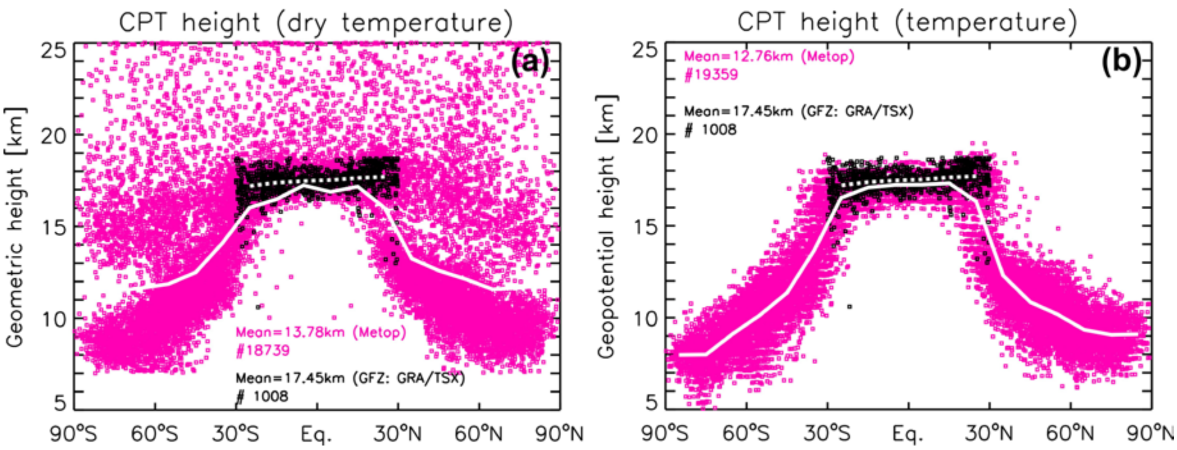

Figure 3: (a) Cold-point tropopause heights based on dry temperatures from GRAS data (red) and GFZ GRACE-A and TerraSAR-X (black, for the tropics only). (b) same as (a), but based on temperatures (red). The solid white lines denote the mean values for 10° latitude bins.

Recommendation: Give the CPT height only for the tropics, e.g. between 30°N and 30°S.

Recommendation: Introduce a further variable for the temperature minimum and the according height over the complete profile.

Remark: Considering the complete test dataset more than 600 CPT_TDRY values are less than 5 km.

As mentioned above the introduction of TPH diagnostic tools are very useful. In addition the tropopause temperatures are also important.

Recommendation: Introduce a further variable for the tropopause temperature for TPH_TDRY, CPT_TDRY, TPH_TEMP, and CPT_TEMP.

Finally Figure 4 shows the zonal mean TPHs from the different diagnostic tools including the independent results from the GFZ data. Beside the different numbers of TPHs the TPH values agree very well in al latitude bands with the exception of TPH_BEND that is generally higher compared with the other results (Figure 4a). If comparing only results when all TPHs could be successful determined (Figure 4b) the agreement in the extra-tropics is even better for TPH_REFR, TPH_TDRY, and TPH_TEMP, but with differences in the tropics (lower TPH_REFR and higher TPH_BEND compared with TPH_TDRY and TPH_TEMP).

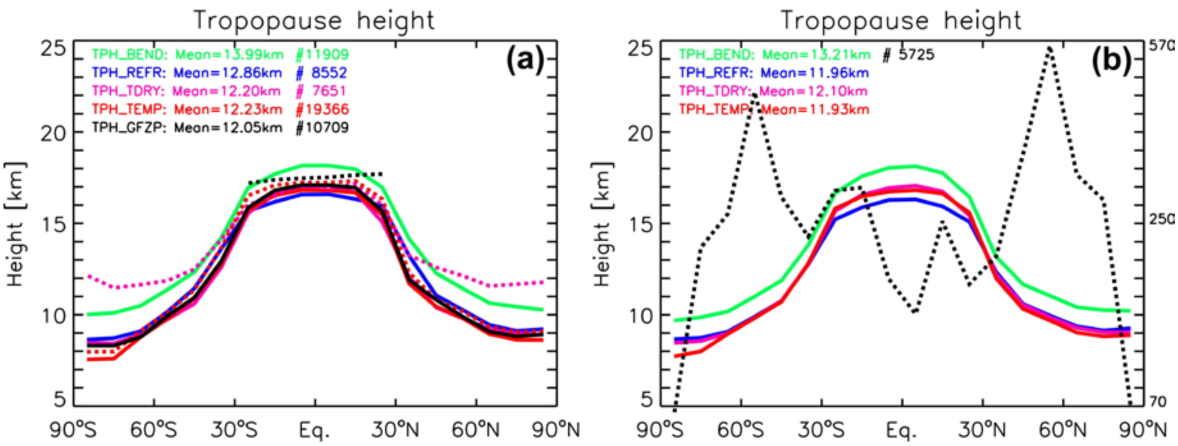

Figure 4: (a) Zonal mean tropopause heights based on different data sets. The dotted lines are the according cold-point tropopause heights. (b) Same as (a), but only based on profiles where all TPHs could be calculated. The black dotted line denotes the number of profiles (right axis).

Figure 5 summarizes the relative number of valid TPHs (flag=0) for the different diagnostic tools as a function of latitude. Beside the CPT heights and TPH_TEMP the other TPHs show a low yield for all latitudes.

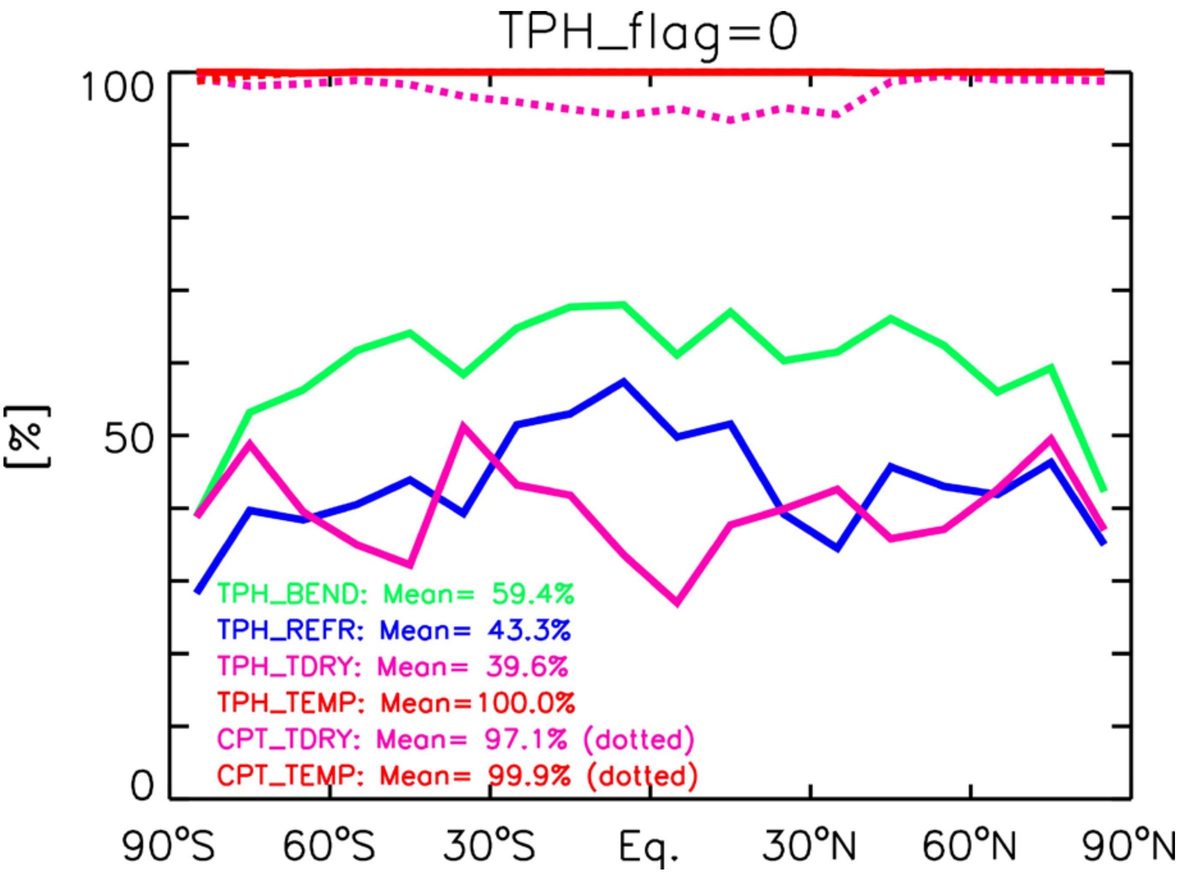

Figure 5: Relative number of valid TPHs (flag=0) according the total number of profiles per latitude bin.

In the following sub-Chapters some details of the TPH diagnostic tools are reviewed mainly with respect to the different settings of the flags that lead to a possible exclusion of the TPH result.

I refer to the ROM SAF documentation Part III: Pre-processor module (pp. 42-53).

3.2.2 TPH based on bending angle (TPH_BEND)

The TPH_BEND tool follows a method introduced by Lewis (2009) that was also applied by the reviewer in a previous study (Schmidt et al., 2010) and showed a good agreement with lapse-rate TPHs based on dry temperatures.

The yield of TPH_BEND in relation to the total number of the test dataset is 59.4%. The reason for exclusion of TPHs according the different flags (1-7) is shown in Figure 6a.

In the following I refer to the documentation of the Pre-processor module.

Page 43:

Formula (5.1): I would suggest some additional tests with the "2a" value, also with lower values than the implemented fixed 35 km. Define this value maybe latitude-dependent?

Flag=1: OK.

Flag=2: If the latitude is missing I would not set it to zero, because then a wrong assignment of TPH and latitude occurs. It would be possible that a low polar TPH is related to the tropics (latitude = 0).

Flag=3 and 4: Flag=4 is responsible for 27.3% of rejected TPHs. There is a clear latitudinal dependence of flag=4 with maximum at the poles.
Could this number be reduced by variation of z_t (25 km or 20 km according location)?
Could this number be reduced by soften the 5 km below the possible TPH value (5% from the CT peak value of logα)?
Maybe the TPH searching algorithm should not stop after the first try, but go ahead in the profile for the next possible TPH?
Maybe the parameter settings should be latitude-dependent?

Page 44:
Flag=5: I would remove this condition because even in the case you find a second tropopause (0.3% in the test dataset) this should not be a criterion for a rejection of the TPH.

Flag=6: For the lower boundary of the possible TPH I would suggest to use the method from Son et al. (2011). They limit the TPH minimum as a function of latitude according the empirical formula:
TPH_minimum=7.5+2.5cos(2ϕ), with ϕ as the profiles latitude. This gives a minimum TPH of 5 km at the poles and a minimum TPH of 10 km at the equator which is reasonable from a climatological view.

Flag=7: The upper TPH limit of 25 km might be too high. Usually in terms of the lapse-rate TPH from temperatures the upper limit is mostly defined by 70 hPa pressure level. Here I would introduce something similar to Son et al. (2011): TPH_maximum=17.5+2.5cos(2ϕ), with ϕ as the profiles latitude. This gives a maximum TPH of 15 km at the poles and a maximum TPH of 20 km at the equator which is also reasonable from a climatological view.

3.2.3 TPH based on refractivity (TPH_REFR)

The yield of TPH_REFR in relation to the total number of the test dataset is 43.3%. The reason for exclusion of TPHs according the different flags (1-7) is shown in Figure 6b.

Page 44:

Flag=1 to 7: In general the same comments than for TPH_BEND are valid. Most of the TPHs are rejected due to flag=3 (8.3%) and flag=4 (34.4%).

3.2.4 TPH based on dry temperature (TPH_TDRY and CPT_TDRY)

The yield of TPH_TDRY in relation to the total number of the test dataset is only 39.6%. The reason for exclusion of TPHs according the different flags (1-7) is shown in Figure 6c.

Page 45:

Flag=1: Here I would suggest having at least continuous data between 8 and 20 km, maybe latitude-dependent.
Because the pressure should be known at this processing step I would recommend limit the tropopause search between 500 and 70 hPa.

Flag=2: This flag rejects the most part of the possible TPHs (45.0%). The lower borders for the profile seems well chosen so I suppose the low number of profiles reaching this values are caused by the retrieval software generating the dry temperatures.

Page 46:

Flag=5: Why do you want reject the tropopause in case of double tropopauses? On the other hand I wonder because the case flag=5 do not occur. This means that there is no second tropopause in the dataset?

Flag=6 and 7: For the case of temperature profiles I would recommend limit the tropopause search between 500 and 70 hPa, also for the CPT.

Remark: Because the Schmidt et al. (2005) algorithm is little complicated the reviewer itself use for the TPH determination from RO data the Reichler et al. (2003) algorithm applied between 500 and 70 hPa.

The yield of CPT_TDRY in relation to the total number of the test dataset is 97.1%. The reason for exclusion of TPHs according the different flags (1-7) is shown in Figure 6e.

It should be noted that more than 600 CPT_TDRY values are less than 5 km.

3.2.5 TPH based on model temperature (TPH_TEMP and CPT_TEMP)

The yield of TPH_TEMP in relation to the total number of the test dataset is 100% (Figure 6d). The only remark here is related to the “negative pressure” on page 47. If this case occurs I would suggest stop processing.

The yield of CPT_TEMP in relation to the total number of the test dataset is 99.9% (Figure 6f). There are no further remarks.

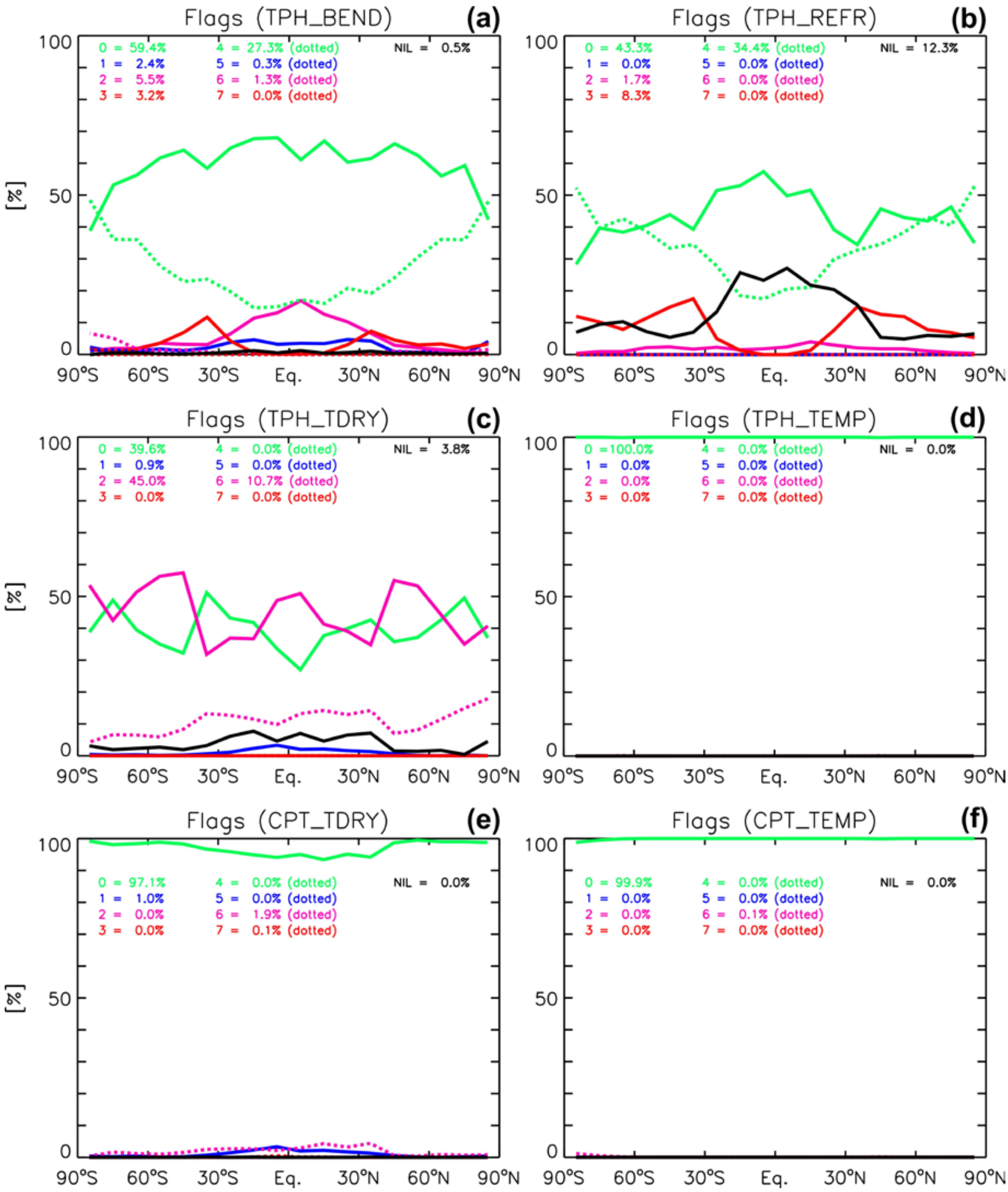

Figure 6: Relative number of flags (0-7) according the total number of profiles per latitude bin for the different TPH diagnostic tools.

4. Conclusions

The introduction of TPH diagnostic tools in ROPP-7.0 is very useful because the TPH is recognised as a parameter for climate change.

The RO technique offers several vertical parameters during the different processing steps containing a different degree of a-priori and/or background information. Therefore from the climate monitoring perspective the calculation of the TPH on the basis of bending angles, refractivity, and temperature is suitable.

During this review different TPH diagnostic tools were tested with a one-month GRAS dataset for April 2013 (over 19 000 occultation events). Based on this dataset a zonal climatology (10° latitude bins) was generated to evaluate the results from a climatological perspective. In addition to that one month (April 2013) of GRACE-A and TerraSAR-X data (about 10 000 occultations) processed at GFZ Potsdam was used to calculate the TPH on the basis of an own and independent method. A similar zonal climatology was provided.

Overall there is a good agreement between the different TPH altitudes but with about 1 km higher TPH_BEND compared with the other TPHs and slightly lower TPH_REFR in the tropics compared with TPH_TDRY.

Several CPT_TDRY heights are partly unrealistic and the searching algorithm should be revised. A limitation of the searching algorithm between 500 and 70 hPa would remove most of the unrealistic values.

The yield of the different TPHs related to the total number differs and is generally low for all TPHs with the exception of TPH_TEMP and the CPT.

I would like to make some suggestions for the TPH diagnostics tools:

1. Experiment with and/or change some (strict) criteria in the single TPH diagnostic tools to optimise the TPH_BEND for a better agreement with TPH_REFR and TPH_TDRY and to get a higher yield of valid TPHs based on bending angle and refractivity: “2a” value, criteria leading to flag=3 and flag=4.
2. For TPH_BEND and TPH_REFR introduce a latitude-dependent upper and lower boundary for a valid TPH (e.g. Son et al., 2011). For temperature-based calculations search for a TPH/CPT between 500 and 70 hPa only.
3. Limit the CPT calculation to the tropics (e.g. between 30°N-30°S) because only in the tropics the CPT is the more reliable tropopause compared with the lapse-rate tropopause.
4. Introduce also the tropopause temperature for TPH_TDRY, TPH_TEMP and the according CPT heights.
5. Do not reject any TPH if double tropopauses occur.
6. An introduction of the height of the temperature minimum (including the minimum temperature itself) would be interesting.

4.1 Acknowledgments

I would like to acknowledge EUMETSAT, DMI, and Met Office for the invitation to this review.

5. References

Fueglistaler, S., A. E. Dessler, T. J. Dunkerton, I. Folkins, Q. Fu, and P. W. Mote, Tropical tropopause layer, Rev. Geophys., 47, RG1004, doi:10.1029/2008RG000267, 2009.

Highwood E. J., and B. J. Hoskins, The tropical tropopause, Q. J. R. Meteorol. Soc., 124, 1579-1604, 1998.

Lewis, H. W., A robust method for tropopause altitude identification using GPS radio occultation data, Geophys. Res. Lett., 36, L12808, doi:10.1029/2009GL039231, 2009.

Randel, W. J., et al., An update of observed stratospheric temperature trends, J. Geophys. Res., 112, D02107, doi:10.1029/2008JD010421, 2009.

Reichler, T., Dameris, M., Sausen, R., Determination of tropopause height from gridded data, Geophys. Res. Lett., 30, doi:10.1029/2003GL018240, 2003.

Santer B. D., et al., Identification of anthropogenic climate change using a second-generation reanalysis, J. Geophys. Res., 109, D21104, doi:10.1029/2004JD005075, 2004.

Schmidt T., Wickert J., Haser A., Variability of the upper troposphere and lower stratosphere observed with GPS radio occultation bending angles and temperatures. Adv. Space Res., 46, 2, 150-161, 2010.

Schmidt T., Wickert J., Beyerle G., Heise S., Global tropopause height trends estimated from GPS radio occultation data. Geophys. Res. Lett., 35, L11806, DOI 10.1029/2008GL034012, 2008.

Schmidt, T., Heise, S., Wickert, J., Beyerle, G., and Reigber, C., GPS radio occultation with CHAMP and SAC-C: global monitoring of thermal tropopause parameters, Atmosph. Chem. Phys., 5, 1473-1488, www.atmos-chem-phys.org/acp/5/1473, 2005.

Schmidt, T., J. Wickert, G. Beyerle, C. Reigber, Tropical tropopause parameters derived from GPS radio occultation measurements with CHAMP, J. Geophys. Res., 109, doi:10.1029/2004JD004566, 2004.

Seidel, D. J. and Randel, W. J., Variability and trends in the global tropopause estimated from radiosonde data, J. Geophys. Res., 111, D21101, doi:10.1029/2006JD007363, 2006.

Shepherd, T.G., Issues in stratosphere-troposphere coupling, J. Meteorol. Soc. Japan, 80, (4B), 769-792, 2002.

Son, S.-W., N. F. Tandon, and L. M. Polvani, The fine-scale structure of the global tropopause derived from COSMIC GPS radio occultation measurements, J. Geophys. Res., 116, D20113, doi:10.1029/2011JD016030, 2011.

6. List of Acronyms

COSMIC	Constellation Observing System for Meteorology, Ionosphere, and Climate
CPT	Cold PoinT (of a temperature profile)
DMI	Danish Meteorological Institute
ECMWF	European Centre for Medium-range Weather Forecasts
EUMETSAT	EUropean organisation for the exploitation of METeorological SATellites
GFZ	German Research Centre for Geosciences
GNSS	Global Navigation Satellite System
GPS	Global Positioning System (USA)
GRACE	Gravity Recovery And Climate Experiment satellite, carrying an RO sounder
GRAS	GNSS Receiver for Atmospheric Sounding (on Metop)
IEEC	Institut D'Estudis Espacials de Catalunya
Metop	Meteorological Operational Satellite
NetCDF	Network Common Data Form
NWP	Numerical Weather Prediction
RO	Radio Occultation
ROPP	Radio Occultation Processing Package (software package produced by ROM SAF)
ROM SAF	Radio Occultation Meteorology (ROM) Satellite Application Facility (SAF) (EUMETSAT)
TerraSAR-X	Earth observation satellite, carrying an RO sounder
TPH	TropoPause Height
UTLS	Upper Troposphere Lower Stratosphere